2023

Spatial Variability in Above Ground Carbon Within an Appalachian Forest

Megan A. Ponczek
West Virginia University, map00033@mix.wvu.edu

Spatial Variability in Above Ground Carbon Within an Appalachian Forest

Megan A. Ponczek, B.A.

Master's Thesis submitted to the Eberly College of Arts and Sciences
at West Virginia University
in partial fulfillment of the requirements for the degree of
Master of Arts in Geography

Dr. Brenden McNeil, Ph.D., Chair

Dr. Edward Brzostek, Ph.D.

Dr. Amy Hessl, Ph.D.

Department of Geology and Geography

Morgantown, West Virginia

2023

Keywords: Forests, forest carbon, Appalachian Plateau, Geographic Information Systems, water availability, logging disturbance

ABSTRACT

Spatial Variability in Above Ground Carbon Within an Appalachian Forest

Megan A. Ponczek

Forests have long been recognized for their provision of air and water quality ecosystem services to society; but more recently, they have become valuable to the carbon credit markets used as a tool for mitigating climate change. Quantifying above ground carbon storage in forest ecosystems is essential for these carbon credit markets and can also provide insight into factors that control the spatial distribution of carbon in forests. The goal of this study is to assess the degree to which three factors: topography, tree species, and legacies of logging, impact the spatial variability in above ground carbon within a 400x500m Appalachian forest plot. Field work spanning 2018 to 2022 resulted in 14,932 surveyed trees with 27 unique tree species, totaling an estimated 2,107,736 kg of above ground carbon content. I used a multiple linear regression model to determine that 14% (Adjusted $R^2 = 0.14$) of the spatial variability in above ground carbon can be explained by variables representing the three factors included in this study. Tree species, represented by their varying wood densities, explained the most variability (Std Beta = 0.39). Potential Evapotranspiration (PET), a variable summarizing the impact of topography on solar radiative plant water demand, was the second strongest (Std Beta = -0.18). Logging has a direct impact on the amount of above ground carbon content; however, the indirect effect of increased abundance of tree species with lower wood density in more recently harvested stands effectively captured this driver of forest carbon within the statistical model. This study highlights the interacting factors that simultaneously control the spatial variability of above ground carbon, and their impact on long-term carbon storage. For instance, in finding that most of the above ground carbon in the plot is in the dense wood of overstory oak species, and not in the less dense wood of the red maple-dominated understory that will likely replace the oaks over time, this study highlights how the "mesophycation" of eastern North American forests toward species like red maple may negatively affect aboveground forest carbon, and thus the carbon market value of this and similar Appalachian forests. To build on this baseline survey and spatial analysis of carbon stocks in this large Appalachian forest plot, we suggest that additional work can measure rates of aboveground carbon sequestration by repeating the tree census, and by working to identify spatial relationships with below ground carbon.

Table of Contents

List of Tables

List of Figures

Supplemental Figures and Tables

1. Introduction

Forests can provide several ecosystem services to society, such as fuel, clean air, and flood control (Shen & Pagliacci, 2023). More recently, the rapidly growing industry of the forest carbon credit market offers potential to purchase emission reduction credits to counterbalance emissions (Van Kooten & Johnston, 2016). Studies of forest carbon provide useful context for market evaluators of forests, as there are multiple factors that contribute to forest carbon distribution and, therefore, translate into emission reductions. Through logging, humans structure the pattern of above ground carbon by removing carbon containing trees from a logged area. In similarly aged forests, the responses of each tree species to climatic and topographic variation in water availability is another likely control on carbon accumulation. By quantifying above ground carbon within forests and studying its spatial pattern, we seek to provide insights useful for carbon markets by evaluating variables that contribute to the spatial variation in above ground carbon. Such variables include logging history, water availability controlled by topography, and tree species differences in wood density.

Locally based factors that impact tree densities are important to consider regarding forest carbon dynamics, which show that younger logged forests are not typically associated with high carbon amounts (Crowther *et. al.*, 2015). Forests develop natural canopy gaps through windfall and other disturbances. Some forest harvest practices, such as clear-cutting, can alter the severity of these canopy gaps and drive a different species into the area as the canopy regrows (Brice *et. al.*, 2020). Early successional trees tend to establish and grow quickly in clear cut areas (Beck & Hooper, 1986). These tree species are typically shade intolerant and are more opportunistic than late successional trees, like oaks (Alexander *et. al.*, 2019). Early successional trees also typically have lower wood densities, as carbon is allocated more for growth as opposed to storage (Piponiot *et. al.*, 2022).

Approximately half of a tree's biomass is carbon (Chojnacky *et. al.*, 2013). Wood tissue density is one of the most important variables when quantifying carbon for a singular tree, next to stem diameter and tree height. Therefore, in trees of the same size, a species with a higher wood density will have more biomass and will store more above ground carbon (Chave *et. al.*, 2009). Through effects on the species that regrow after a clearcut forest harvest, the logging history of a forest will often be the largest driver in overall carbon content (Chave *et al.*, 2009). Specifically, recently logged areas often have lower above ground carbon content because they have both smaller regrowing trees and are comprised of early successional species with lower wood density.

The topography of a landscape can influence water and nutrient availability, as well as the overall species composition of a forest. For instance, slope aspect plays an important role in water regimes. Equatorial facing slopes experience more solar radiation, increasing plant evapotransipirative water demand, and creating a microclimate which favors drought tolerant species (Fekedulegen *et. al.*, 2003). GIS-enabled assessments of solar radiation and plant water demand can directly quantify the effect of topography upon forest species composition and rates of carbon accumulation (Fekedulegen *et. al.* & Dyer, 2004). In fact, in mesic temperate forests, patterns of water available for plant growth are more strongly controlled by topographic variations in solar radiation, and not by topographic variations in drainage (Dyer, 2009). Thus, by affecting

growth rates, topography, in the form of solar radiative water demand, is likely to impact the spatial variability of above ground carbon in mesic temperate forests.

The purpose of this study is to map and analyze the spatial variability in above ground carbon content within the 18-hectare (44.5-acre) WVU Forest Megaplot at Summit Bechtel Reserve (SBR), located in Fayette County, West Virginia. I focus on three factors that affect spatial variability: past logging history, topographic variation in plant water demand, and species differences in wood density. I will use this information to answer the research question: To what degree do the three factors control the spatial variability of above ground carbon storage?

2. Study Area

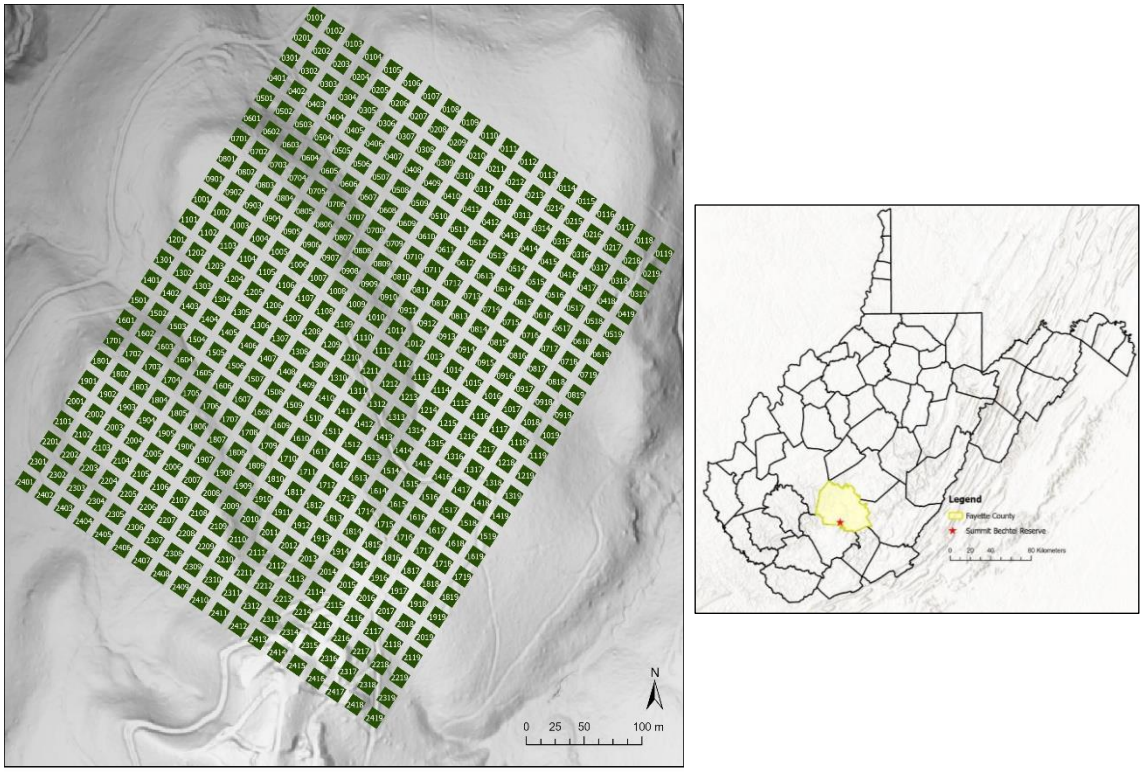

Figure 1: 496 sub-plots at the WVU Forest Megaplot at SBR (Summit Bechtel Reserve)

The study area is the WVU Forest Megaplot at SBR, a predominately deciduous forest in Fayette County, West Virginia (Figure 1). The megaplot is located on the Summit Bechtel Reserve (SBR) property, a national scouting camp, which was established in 2009 and holds the U.S. National Scout Jamboree (Deskins, 2019). There are 456, 20 m^2 sub-plots, that make up the ~18 hectares (44.5 acres) of the megaplot. Fayette County receives an average of 1215 mm of precipitation spread equally through the year with temperatures varying between -0.1 and 21.7º C (NOAA, 2023).

In the mid-1990s, a logging event took place in the southern corner of the megaplot (Figure S1). This area has since been undisturbed and created a forest cover that is significantly denser

than the rest of the megaplot. An aerial image from 1996 georeferenced to the current infrastructure of the megaplot indicated that 48 of the 456 sub-plots are impacted from the mid-1990s logging disturbance (Figure S1). Therefore, stand age is defined by two separate logging disturbances, creating three age cohorts. The younger stand was established in the mid-1990s, the older stand was likely logged in the middle of twentieth century, and there are four large legacy trees that appear to predate the mid-twentieth century logging event.

There are four soil types present in the megaplot: clifftop channery silt loam (ClE), Leyland Dekalb-Guyandotte complex (LeF), Kaymine-Rock outcrop complex (KrF), and Highsplint channery loam (HgE). All soil types are well-drained and stony and have medium to high runoff classes (*Soil Survey Staff*, 2023). LeF makes up the lower elevations and the valley bottoms in the megaplot, while ClE makes up the higher elevations and ridgetops. KrF and HgE make up a small portion of the southern region of the megaplot in the highest elevations (Figure S2).

3. Methods

3.1 Field collection

The dataset consists of information on each tree greater than or equal to 5 cm within each of the 456 20x20m sub-plots in the 400x500m megaplot (Figure 1). The survey date, sub-plot number, tree ID number, species ID, diameter at breast height (DBH), as well as the map distance (to the nearest 0.05m), and directional bearing from the northeast sub-plot corner were recorded for each tree (Table S1). The basal area (in cm^2) is calculated from the DBH. The coordinates of each tree were obtained by applying trigonometry to the precise (survey grade GPS) coordinates of the corner posts in each sub-plot. The survey dates range from 2018 to 2022 where multiple teams of WVU researchers assisted. There are also 30 sub-plots originally surveyed in 2018 that were resurveyed in 2022. The most recent data from 2022 replaced the 2018 data in the final dataset.

There were 139 trees where the survey team could not identify the species, so they were classified as unknown (UNKN). The number of UNKN trees is a small fraction of the total surveyed trees and does not strongly impact above ground carbon amounts. The UNKN trees were typically small, and are likely OXAR, CAGL, or CAOV as these species were most confused during field work collection. For hardwood species that are not explicitly noted in Table 4 of Jenkins *et. al.*, the beta value parameters for mixed hardwood were used (2003). The species ID follows the naming convention of the USDA Plants database (USDA & NRCS, 2023).

3.2 Biomass and carbon calculation

To calculate biomass and carbon from DBH values, I assigned the appropriate set of beta value parameters found in Table 4 from Jenkins *et. al.* (2003). Biomass was then found using the provided biomass formula also in Table 4 of Jenkins *et. al.* (2003), where *bm* is the total amount of aboveground biomass in kg for trees with 5 cm DBH and greater:

$$bm = Exp(\beta_0 + \beta_1 ln\text{DBH}) \quad \text{(equation 1)}$$

Per the conclusions from Chojnacky *et. al.*, there is no significant difference between their biomass estimations and the generalized biomass estimations from Jenkins *et. al.* (2013, 2003). It is recommended that the set of formulas found in Chojnacky *et. al.* or Jenkins *et. al.* can be used if total above ground carbon is the objective, which is the case of this study (2013, 2003). Once biomass was calculated, I calculated above ground carbon by halving the above ground biomass.

3.3 Spatial Variables

The dependent variable in this study is total above ground carbon content in each 20x20m sub-plot, which was found by halving the biomass of every tree, and then totaling the above ground carbon for each sub-plot (Chave *et. al.*, 2009). Tree species impacts on above ground carbon content are inherent in the species-specific parameters within the allometric formula used to calculate above ground carbon (equation 1, Chave *et. al.*, 2009). These parameters summarize measured species differences in wood density, but also measured scaling relationships among DBH with tree height and volume. To directly assess the role of wood density, I used literature values of wood density reported by Zanne *et. al.* (2009). Specifically, I calculated the weighted average wood density for each sub-plot by multiplying the wood density value of each species by its relative proportion of total carbon in the sub-plot.

Water deficits, physical environmental changes, and disturbance impact competition relationships between species. These interactions cause shifts in niches and are not dependent on one driver alone, but a combination of them (Dyer & Hutchinson, 2019). The methods of Dyer (2009) rely on solar radiation maps to identify landscape-scale variability in plant water demand. Following these methods, I used a water balance model to calculate the PET, AET, and then the deficit for each sub-plot. I explored deficits and soil AWC as a possible variable to use in spatial analyses, but they did not add any explanatory power in the statistical model, likely because of the imprecision of soil water storage values (Figure S2). Solar radiative water demand is affected by topography and accounts for slope, elevation, aspect, and topographic shading when calculating PET (Dyer, 2009).

The age of a forest is often the most important factor that controls forest carbon content (Piponiot *et al.*, 2022). When I performed exploratory point density analyses for above ground carbon, there were four large "legacy" trees exceeding 90 cm DBH that weighed heavily on the analysis and made it difficult to detect nuanced spatial patterns. Because of the large nature of the dataset, which consists of 14,932 trees, the removal of the legacy trees did not significantly bias statistical analyses. The stand age values of 25

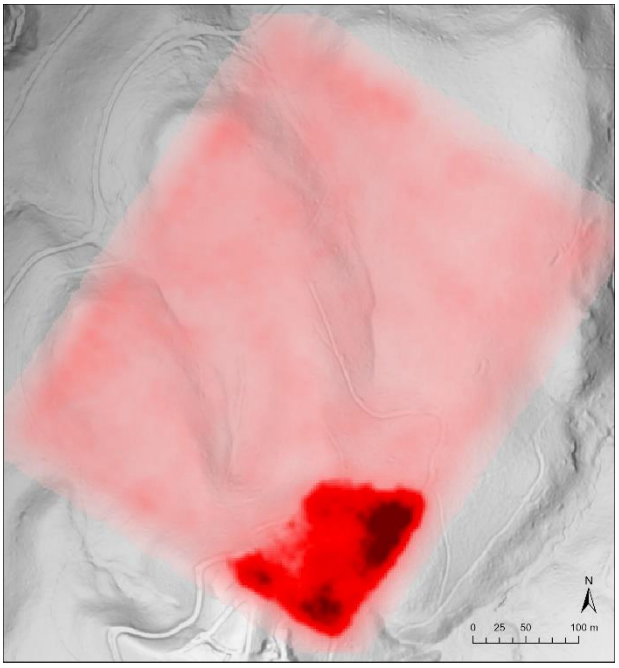

Figure 2: Point density of trees using a 20-meter neighborhood to highlight density of the younger stand that underwent logging in the mid-1990's.

and 80 years were chosen to represent the time frame (relative to the mid-point of our sample in 2020) of the estimated logging disturbances in ~1940 and ~1995 (Figure S1).

3.4 Statistical and spatial analyses

I utilized univariate, and multiple linear regression analyses in JMP statistical software version 16.0.0 to determine the degree to which each of the three independent variables (wood density, PET, stand age) relates to the above ground carbon content measured in each sub-plot. By scaling to the sub-plot level, outlier bias is minimized, and provides more robust measures of spatial pattern (Smith *et. al.*, 2004). I accounted for spatial autocorrelation using Global Moran's I spatial autocorrelation tool and performed all mapping analyses in ArcGIS Pro version 3.0.2.

4. Results

4.1 Tree species and above ground carbon

Within the 456 sub-plots there are 14,932 trees with 27 unique species and the unknown species (UNKN) category (Table 1). The total above ground biomass calculated for the megaplot is 4,215,472 kg, and the total above ground carbon present in the megaplot is 2,107,736 kg. The top five most abundant species make up ~71% of the 14,932 trees present in the megaplot and 82% of the total above ground carbon. Red maples are distributed evenly through the megaplot (Figure 3) and make up 40% of the total trees, but only 26% of the biomass. Red and black oaks are more common in the canopy overstory and on ridges (Figure 4) and comprise 40% of the biomass. The variation in species-specific above ground carbon within these species can be explained via basal area. Though red maples are the most abundant species, their average basal area per tree is 284 cm^2 and average above ground carbon is 91 kg, while the red oak's average basal area is 1214 cm^2 and average above ground carbon is 532 kg per tree (Table 1). Especially relative to other species, the concentration of tulip trees is high in the younger stand that underwent logging in the mid-1990's (Figures 5 & 6). However, the smaller tree sizes and relatively low wood density of tulip trees (Table 1) are related to generally lower amounts of total above ground carbon in the most recently logged region (Figure 7).

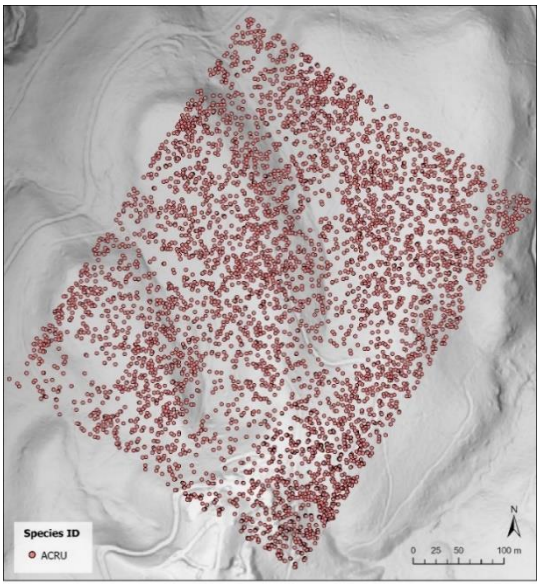

Figure 3: The 6,017 Red maples present in the megaplot

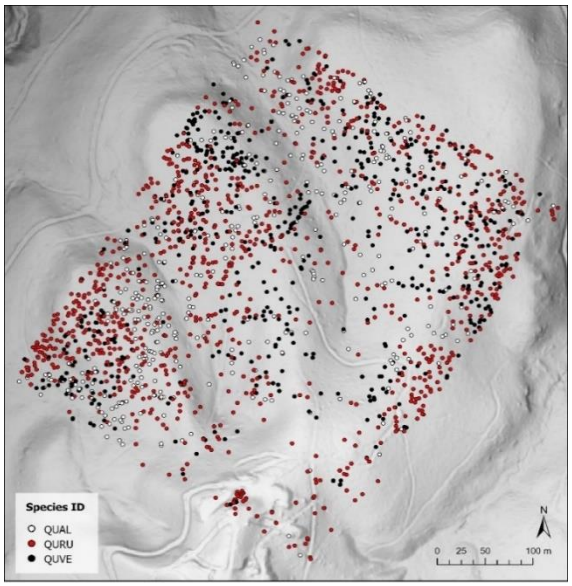

Figure 4: The most populous oak species present in the megaplot; 1,041 red oaks, 590 black oaks, and 405 white oaks. Oaks are most concentrated on the south facing slopes and ridges where evaporative water demand is higher.

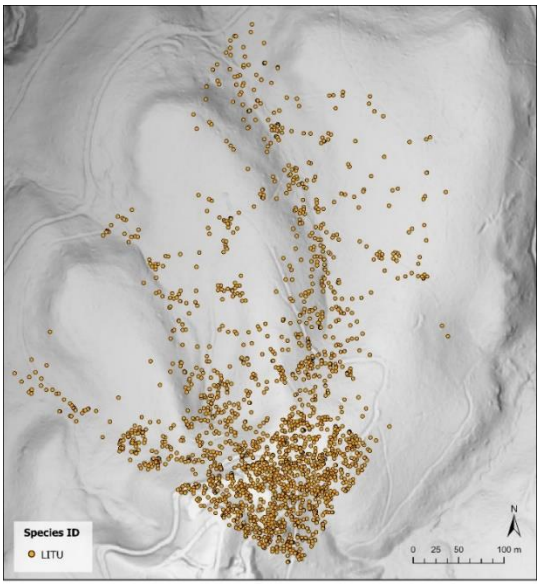

Figure 5: The 2,118 tulip trees present in the megaplot. 48% (1,024) are in the southern logged region of the mid-1990's

Table 1: 27 tree species with scientific and common names, mycorrhizal association (AM = arbuscular mycorrhizae and EM = ectomycorrhizae), wood density (g/cm^3) from Zanne *et. al.* (2009), the number of stems present, total basal area (cm^2), total above ground carbon (KgC), and the beta values used in the biomass calculation from Table 4 of Jenkins *et. al.* (2003).

Species ID	Scientific Name	Common Name	Mycorrhizal Association	Wood Density	Stems	Total basal Area	Total Above Ground Carbon	β_0	β_1
ACPE	*Acer pensylvanicum*	Striped maple	AM	0.44	20	2471	780	-1.9123	2.3651
ACRU	*Acer rubrum*	Red maple	AM/EM	0.49	6017	1708895	548029	-1.9123	2.3651
ACSA	*Acer saccharum*	Sugar maple	AM	0.56	441	92152	31441	-2.0127	2.4342
ALRU	*Alnus rubra*	Red alder	AM	0.37	1	21	3	-2.2094	2.3867
AMAR	*Amelanchier arborea*	Downy Serviceberry	AM	0.66	7	1088	248	-2.48	2.4835
ASTR	*Asimina triloba*	American Papaw	AM	0.39	1	48	7	-2.48	2.4835
BELE	*Betula lenta*	Black birch	EM	0.60	293	32812	8703	-1.9123	2.3651
CACA	*Carpinus caroliniana*	American hornbeam	EM	0.32	1	62	9	-2.48	2.4835
CAGL	*Carya glabra*	Pignut hickory	EM	0.58	366	155296	58798	2.0127	2.4342
CAOV	*Carya ovata*	Shagbark hickory	EM	0.64	84	45329	17483	2.0127	2.4342
COFL	*Cornus florida*	Flowering dogwood	AM	0.64	55	2273	331	-2.48	2.4835
FAGR	*Fagus grandifolia*	American beech	EM	0.56	446	33241	8830	-2.5095	2.6175
FRAM	*Fraxinus americana*	White ash	AM	0.55	6	3208	980	-2.48	2.4835
LITU	*Liriodendron tulipifera*	Tulip tree	AM	0.40	2118	726686	191069	-2.48	2.4835
MAAC	*Magnolia acuminata*	Cucumber magnolia	AM	0.46	341	103182	27883	-2.48	2.4835
NYSY	*Nyssa sylvatica*	Black gum	AM	0.46	731	189829	54835	-2.48	2.4835
OXAR	*Oxydendrum arboreum*	Sourwood	AM	0.50	435	44659	9172	-2.48	2.4835
POGR	*Populus grandidentata*	Bigtooth aspen	AM	0.36	26	11071	2737	-2.48	2.4835
PRSE	*Prunus serotina*	Black cherry	AM	0.47	123	35532	9209	-2.2094	2.3867
QUAL	*Quercus alba*	White oak	EM	0.60	405	320395	132069	-2.48	2.4835
QUPR	*Quercus prinus*	Chestnut oak	EM	0.57	795	306121	120097	-2.0127	2.4342
QURU	*Quercus rubra*	Red oak	EM	0.56	1041	1264356	554837	-2.0127	2.4342
QUVE	*Quercus velutina*	Black oak	EM	0.56	590	680123	292007	-2.0127	2.4342
ROPS	*Robinia pseudoacacia*	Black locust	AM	0.66	20	5905	1474	-2.0127	2.4342
SAAL	*Sassafras albidum*	Sassafras	AM	0.42	380	85635	20633	-2.48	2.4835
TIAM	*Tilia americana*	American basswood	EM	0.32	9	4569	1230	-2.48	2.4835
TSCA	*Tsuga canadensis*	Eastern hemlock	EM	0.38	41	10536	2338	-2.48	2.4835
UNKN	(unidentified species)	(unidentified species)	N/A	0.50	139	42400	12500	-2.5384	2.4814

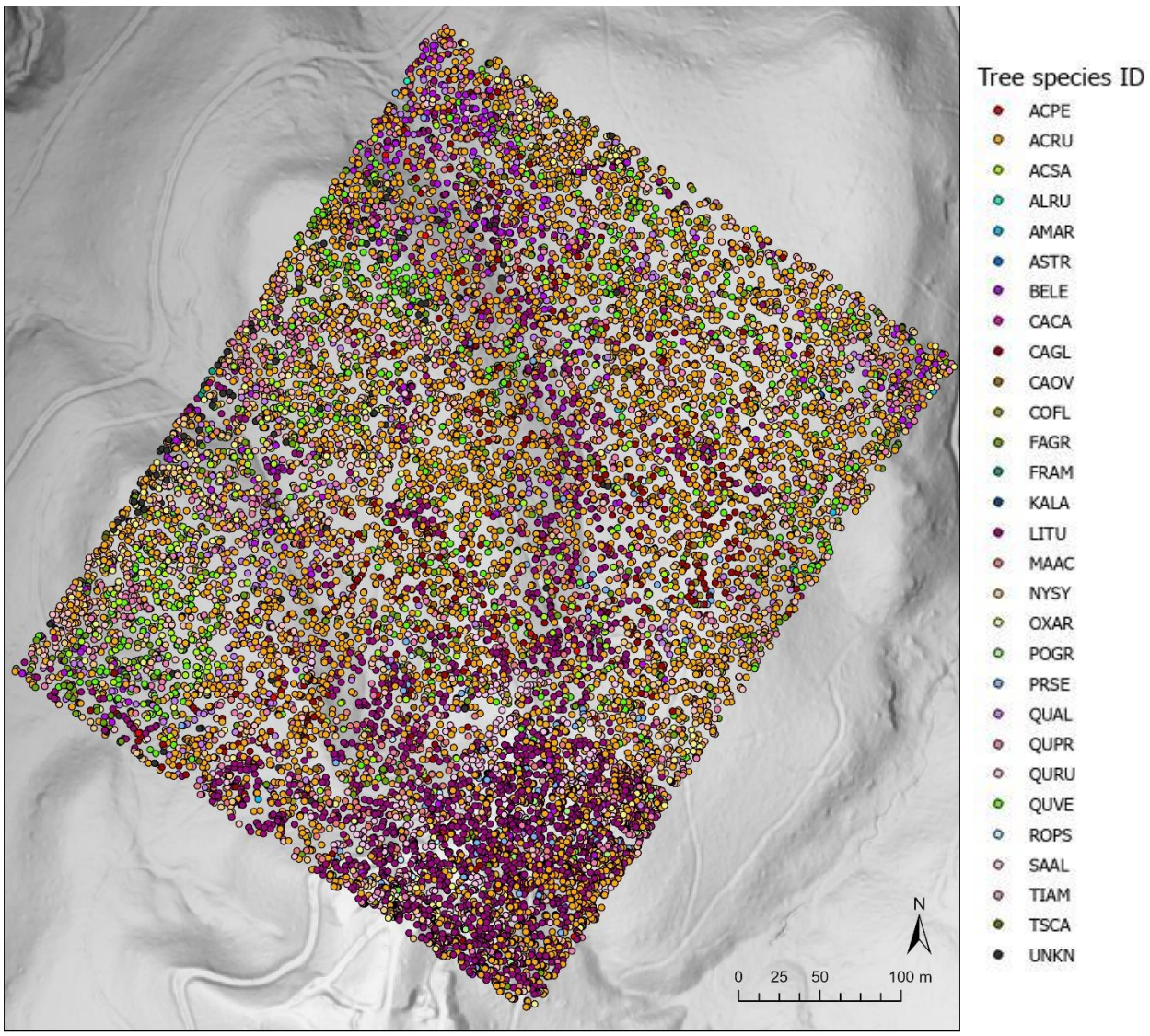

Figure 6: 27 unique species that comprise the 14,932 trees present in the WVU Forest Megaplot at SBR. The 139 trees with unknown species ID (UNKN) are included.

The above ground carbon content is not distributed randomly, supporting the notion that there are spatial factors that contribute to its distribution. After executing the Global Moran's I tool within ArcGIS Pro using a default distance parameter of 20 meters, I found the total above ground carbon figures to be spatially autocorrelated with a z-score of 2.008, and a p-value of 0.044. There were 4 trees in the megaplot that exceeded 90 cm DBH, likely because they were left as seed or shade trees during the forest harvest that likely occurred in the middle of the twentieth century. Preliminary density analyses showed that these four trees greatly influenced the spatial pattern, so I removed them to prevent biases in spatial above ground carbon and basal area analyses (Figure 7). The northeastern valley within the megaplot and along the ridgetops where the northeastern and southwestern valleys meet have higher concentrations of above ground carbon (Table S2). The southern corner of the megaplot contains the lowest concentrations of above ground carbon, consistent with the location of the 1996 logging disturbance (Table S2).

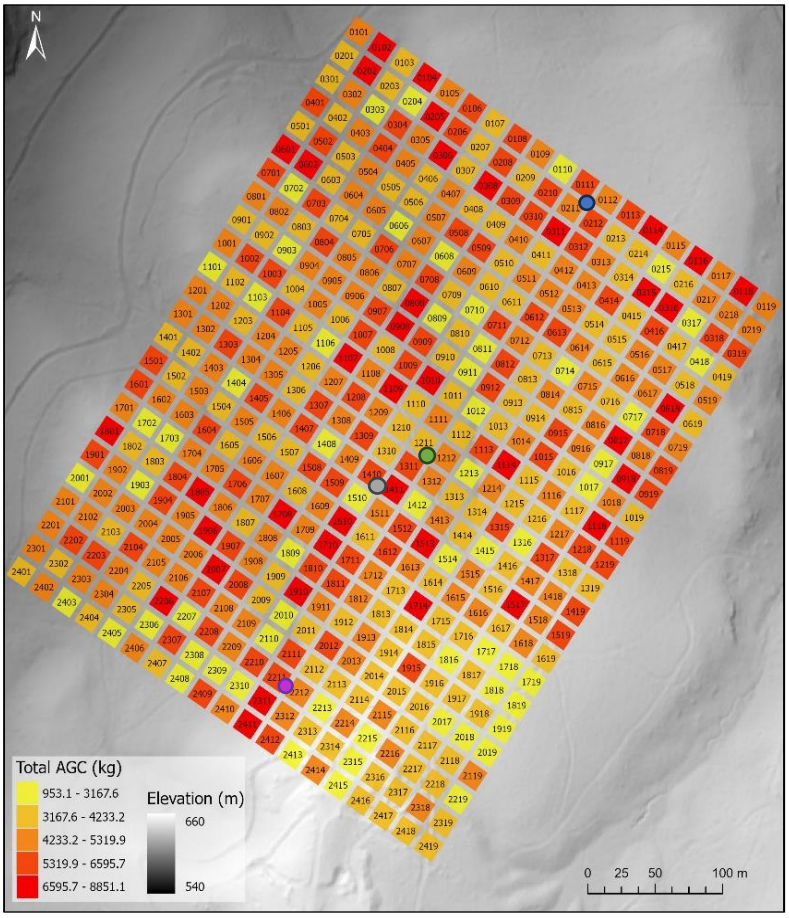

Figure 7: Total above ground carbon for each sub-plot within the megaplot. The colored circles represent the location of the 4 legacy trees:

- 0111-13, QURU, 9513 KgC
- 1211-25, ACRU, 6203 KgC
- 1410-19, ACRU, 13101 KgC
- 2211-11, QURU, 7866 KgC

4.2 Spatial controls on above ground carbon

I examined the PET, stand age, and wood density variables against the total above ground carbon and found that the strongest correlation is between the stand age and the wood density (r = 0.72). This strong correlation explains and accounts for both the younger, shade intolerant species in the younger stand, and the older stand which contains the denser oak species. However, the wood density had the strongest correlation with above ground carbon content; therefore, it was utilized in the multiple linear regression model (Table 2). The relationship is also bolstered due to the mean above ground carbon content being higher in sub-plots with the older stand (Figure 8). Further, stepwise multiple regression was also used to explore explanatory spatial variables on above ground carbon content. Once wood density is added to the regression model, PET is the next highest explanatory variable. No other variables improved model performance, as the final model including PET and wood density had the lowest AIC of any possible model.

Table 2: Correlation values (Pearsons *r*) between variables. AGC = Above Ground Carbon (KgC). Values significant at p = 0.05 are in **bold**.

	Total AGC	PET	Stand Age
PET	-0.03		
Stand Age	**0.30**	-0.02	
Wood Density	**0.36**	**0.23**	**0.72**

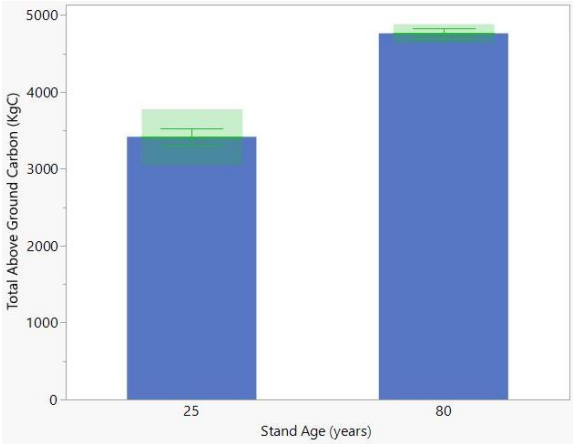

Figure 8: Relationship between stand age and the mean above ground carbon content with the standard error of the mean as the error interval. R^2 = 0.094, P-Value = < 0.01

The multiple linear regression model indicates that 14% (adjusted R^2 value = 0.14) of spatial variability in above ground carbon can be explained by wood density (Std Beta = 0.39) and PET (Std Beta = -0.12). As expected, sub-plot averaged wood density explains the most variance of spatial variability in above ground carbon (Figure 9). The secondary effect of PET indicates that above ground carbon is lower in sub-plots with greater water demand (Figure 10 and Figure S3).

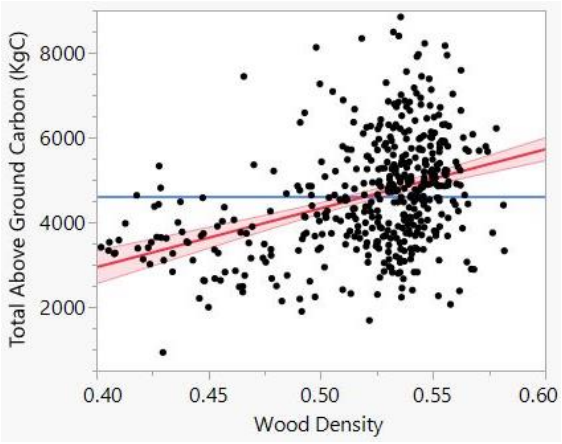

Figure 9: Univariate linear regression result between the total above ground carbon and wood density (g/cm^3). R^2 = 0.13, P-Value = < 0.05.

5. Discussion

5.1 Stand age

This study highlights how above ground carbon in forests changes with stand age. The lowest above ground carbon concentrations are located within the region logged in the mid-1990's (Figure 7 & Figure S1). This region is also the densest in terms of number of stems per sub-plot (Figure 2), confirming that dense forested regions are not necessarily associated with high above

ground carbon content (Crowther *et. al.*, 2015). Further, when the younger stand is excluded from analyses, a Hot Spot Analysis (Getis-Ord Gi*) indicates no significant clustering of cold or hot spots with respect to above ground carbon concentration, indicating that in the presence of a logging disturbance, spatial analyses are statistically impacted by lower concentrations of above ground carbon in logged regions (Figure S7 & Figure S8).

As Table 1 suggests, oak species contain the highest fraction of biomass wihtin the megaplot and prefer areas with more dry soils (Xu *et. al.*, 2019). The allometry of the biomass fomula implies that oaks hold more above ground carbon per unit basal area than any other species, explaining the highest correlation between wood density and above ground carbon. While other studies have found climate variables to explain much of the size distribution in their study areas (Piponiot *et al.*, 2022), they also note that disturbances can have localized effects that are important at landscape-level scales like this study. In our study, the clear cut in the 1990s caused opportunistic species to establish, including red maple, tulip trees, and sassafras (Alexander *et. al.*, 2021). These shade intolerant and intermediate shade tolerant species have lower wood densities than late successional oak species because they allocate carbon for growth. This strongly affected our above ground carbon data, as evidenced when comparing wood densities of the young and old stand (Table 2 & Figure 8).

5.2 Solar radiation and water deficits

Once the statistical model accounted for the combined effect of stand age and species composition, it suggests a negative effect of topographic PET upon the accumulation of above ground carbon. This suggests that topographic variations in water demand impact how fast trees accumulate carbon (Dyer, 2004). It is notable that this secondary effect of PET on aboveground carbon stocks was not statistically significant in the univariate correlation, likely because of a countervailing significant positive correlation among PET and wood density (Table 2). Indeed, as illustrated in Figure 4 and Figure S3, sub-plots with higher PET tended to be on south-facing ridges that contained greater abundances of trees (especially oaks) with higher wood densities (Xu *et. al.*, 2019 & Dyer, 2009).

5.3 Vegetation dynamics

There are clear spatial patterns in species abundances in the megaplot (Figures 3-6), which ultimately affect the spatial pattern of aboveground carbon. In addition to the strong effect of stand age on species composition, topographic variations in solar radiation drive water availability, and thereby, create niches for species that differ in their drought tolerances (Canham et al. 2006 & Dyer, 2009). In Appalachian forests specifically, opportunistic trees such as tulip trees (LITU) establish and grow in clear cut areas (Beck & Hooper, 1986). This can be evidenced in Figure 5 where the abundance of tulip trees strongly correlate with the mid-1990's logging disturbance. Red maples are unique in that their occurrence has no clear spatial pattern within the megaplot, but their relative abundance does tend to be higher in sub-plots with greater PET (Figure 3, Figure S6).

Following European settler colonization, fire suppression increased, which drove dominance towards mesophytic, shade intolerant and intermediate shade tolerant species

(Nowacki & Abrams, 2008). However, a recent study suggests that mesophication is not entirely unique to the twentieth century, as evidence of it can be found via witness trees that contain fire scars after settler colonization and before fire suppression in southeastern Ohio. Multiple factors led to instances of mesophication in pre settler colonization as opposed to one, particularly, changes in land use and water availability (Dyer & Hutchinson, 2019). These results coincide with the niche of trees present in the younger stand logged in the mid-1990's (Figure S1 & Figure 5). A previous study evidenced that higher PET and longer growing seasons will become more common in Appalachian forests, and land-use changes, such as clear-cut logging, can amplify these impacts (D'Orangeville *et. al.*, 2018). These results are bolstered in this study as PET was the strongest topographic variable. While growing seasons are becoming longer, climate change is causing increased precipitation in the Appalachian Plateau (Gaertner *et. al.*, 2019). It is expected that the shift towards mesophytic species will continue and may become more exaggerated as the climate continues to increase. To store more carbon persistently over time, our results suggest we should undertake forest management to promote the growth of oak species.

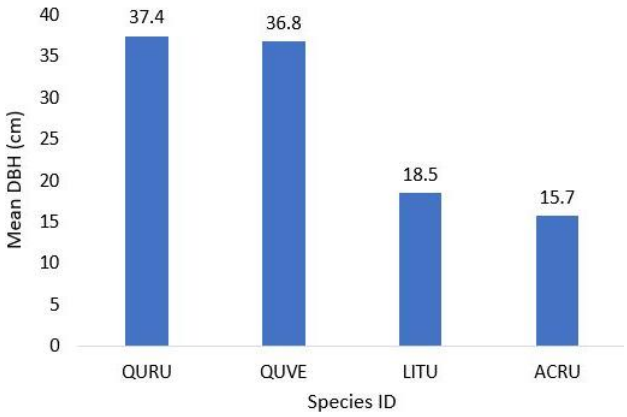

Figure 10: Mean DBH of red oaks, black oaks, tulip trees, and red maples.

However, the trees of the younger stand appear to be sequestering above ground carbon faster than the trees of the older stand in the short-term (Figure 8). A long-term study at the Harvard Research site found that red oak's total biomass increased from 30% to 34% and red maple biomass decreased from 17% to 14% from 1992 to 2013 (Finzi *et. al.*, 2020). A reason that can be speculated from this is the increase of mortality in red maples and tulip trees which intense herbivore browsing and wind throw disturbances contribute to (Abrams, 1998, Hanson *et. al.*, 2001). This results in red maples and tulip trees being amongst the smallest and lowest above ground carbon storing species in the megaplot (Figure 10).

While the trees in the younger stand may be growing and sequestering carbon faster, oak species may still contribute more to the total above ground biomass and carbon in the long-term. Therefore, disturbances such as logging and an increasing climate change species composition to favor species such as maples and tulip trees, which can lessen overall above ground carbon storage in the long-term.

5.4 Megaplot resurvey

Table 3: Current data obtained from the 30 sub-plots of the 2022 resurvey.

	Tree Count	**Dead Trees**	**Total AGC (kg)**
2018 Survey	1,127	111	328,133
2022 Resurvey	1,206	264	361,745
Increase/Decrease	+79	+153	+33,612

We conducted a partial resurvey of the megaplot in 2022, 5 years after the initial survey in 2018, and this can give partial insight into carbon storage and mortality rates within the megaplot. Of the 30 sub-plots that were resurveyed, 1,127 living trees with DBHs greater than 5 cm were recorded in 2018, and 1,206 living trees were recorded in 2022 for a net positive ingrowth of 79 trees. 111 trees were recorded dead in 2018, and 264 were recorded dead in 2022. The percentage of dead trees in 2018 increased from 9.8% to 21.8% in 2022, even with the addition of 79 new trees large enough to be included in the survey. While mortality increased from 2018, it does not outweigh increasing tree size as there was a gain of 33,612 kg of above ground carbon content in 5 years (Table 3). The resurvey was conducted at the same tree-level metrics as the initial survey, including the species of trees that died from 2018-2022. This inclusion of species mortality may help contribute to aNPP estimates with the completion of the resurvey and provide a more in-depth insight of carbon storage capacity amongst species (Dye *et. al.*, 2016).

5.5 Future directions – linking above- and below-ground interactions

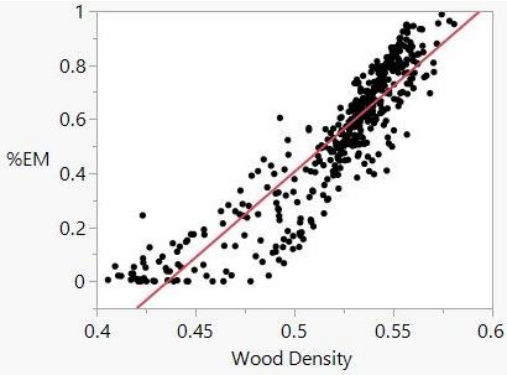

Figure 11: Representative relationship between %EM dominated sub-plots and wood density (g/cm^3). $R^2 = 0.82$.

Wood density is a useful metric of how each species differs in above ground carbon allocation. Surprisingly, it also strongly relates to the strategy that each species uses to allocate carbon to belowground mycorrhizae (Figure 11). Ectomycorrhizal (EM) species retain more carbon than arbuscular mycorrhizal (AM) species (Rygiewicz & Andersen, 1994), which suggests biogeographic traits for long term carbon storage. For example, red oaks (EM) hold a competitive advantage due to their high water-use efficiency and rates of photosynthesis, which assist them in storing carbon longer and more efficiently than other species (Finzi *et. al.*, 2020). While red maples are classified as having an AM mycorrhizal relationship, they display genotypic variation in both upland and bottomland species, and they can act as both an early and late successional species (Abrams, 1998). Additionally, their low lignin litter content is more comparable to an EM species, like oaks (Nowacki & Abrams, 2008). Further, their wood density falls between those of AM and EM species (Table 1) and contains no distinct spatial pattern, compared to oaks or tulip trees (Figures 3, 4, & 5). Because soils store more carbon than both the vegetation and atmosphere globally, it is vital to incorporate in studies that evaluate forest carbon dynamics. This is especially true under the implications of climate change where soil warming significantly contributes to soil carbon loss (Finzi *et. al.*, 2020). I suggest further research at the SBR megaplot can productively seek to further identify linkages among above- and below-ground carbon interactions.

While my model indicated that wood density was the highest explanatory variable, each variable in this study contributes to the spatial pattern of above ground carbon. The three age cohorts' structure above ground carbon content, and the disturbance history ultimately determines the total above ground biomass and carbon content in a forest. Water availability has a strong effect

on species composition and growth. Results of my study conform to the results of a previous study that also indicate ecological responses to multiple drivers in forests (Dyer & Hutchinson, 2019). This study sheds light on the intertwining variables that impact forest carbon content, a complete resurvey of the megaplot will allow for the calculation of carbon storage rates and a more accurate forest model to measure forest carbon offsets in the carbon market (Van Kooten & Johnston, 2016).

6. Conclusion

This study examines the spatial variability of above ground carbon in the WVU Forest Megaplot at SBR by analyzing three factors: topographic variation, tree species differences in wood density, and stand age following separate logging events in the middle and late twentieth century. Using multiple linear regression analysis, these variables explain 14% (Adjusted R^2 = 0.14) of the spatial variability in above ground carbon. Tree species, represented by their wood densities, explained the most variability (Std Beta = 0.39). A topographic PET variable was the second strongest (Std Beta = -0.12). Though the average wood density had the strongest statistical correlation with above ground carbon content, the disturbance history ultimately determines the total above ground biomass and carbon content in a forest. The species of the tree itself is dependent on soil moisture and water deficits which impact how much above ground carbon can be stored per unit of basal area. The results of my study highlight that there are multiple factors that simultaneously contribute to the spatial variability of above ground carbon. A complete resurvey of the megaplot is planned to be completed in upcoming years to obtain more knowledge on carbon storage rates, mortality rates, and below ground carbon interactions to provide a more accurate framework for forest carbon market evaluators.

7. Supplemental Figures and Tables

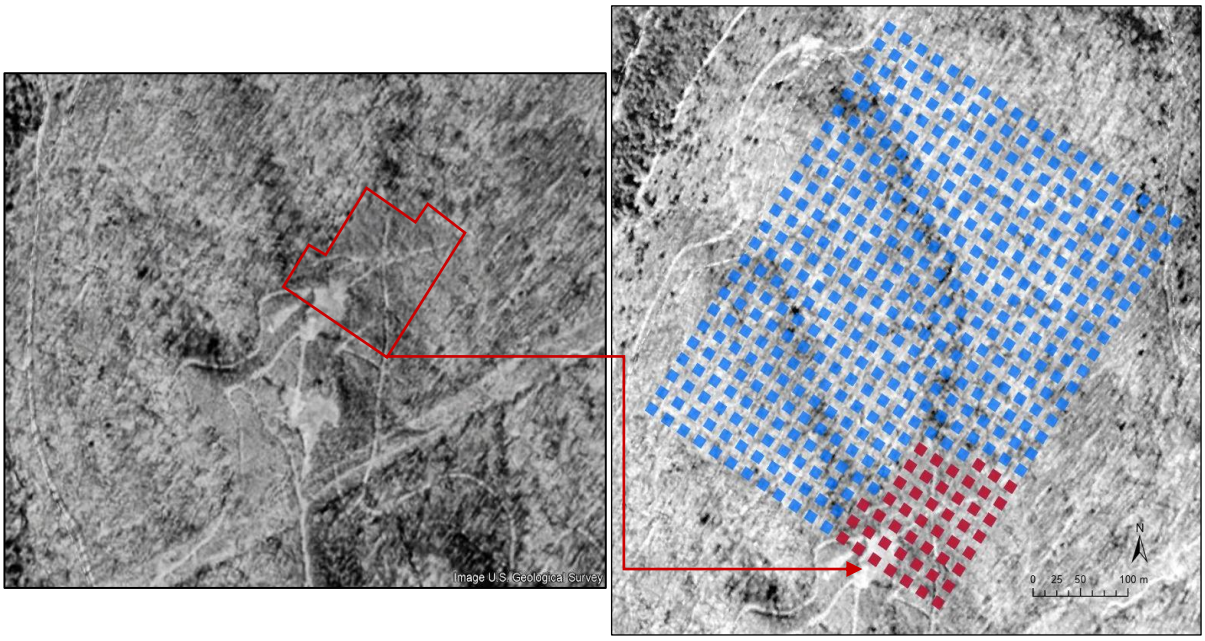

Figure S1: 1996 aerial imagery of logging disturbance (left) with sub-plots impacted (right)

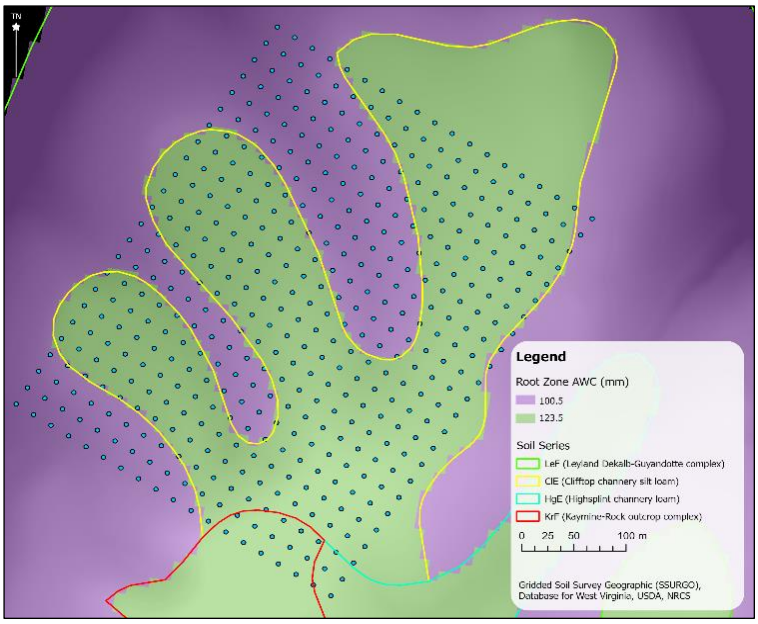

Figure S2: Soil series and root zone AWC within the SBR megaplot (Soil Survey Staff, 2020, 2022, & 2023)

Table S1: Field survey data collected for each surveyed tree.

Data Collected for Each Tree	Data Description
Survey Date	Date each tree was surveyed
Sub-plot Number	Row and column number of each sub-plot (i.e., 0101)
Tree ID Number	Sub-plot number and the individual tree number in the sub-plot (i.e., 0101-05)
Species ID	Four-letter acronym of each tree's scientific name (i.e., ACRU for *Acer rubrum*, or red maple)
DBH	Measured to nearest cm, 1.3 meters from the base of the tree
Distance	Measured to nearest 0.05 m from the northeast corner post of each sub-plot, does not exceed 28.28 m
Directional Bearing	Measured in degrees from the northeast corner post, between 130 and 220 degrees

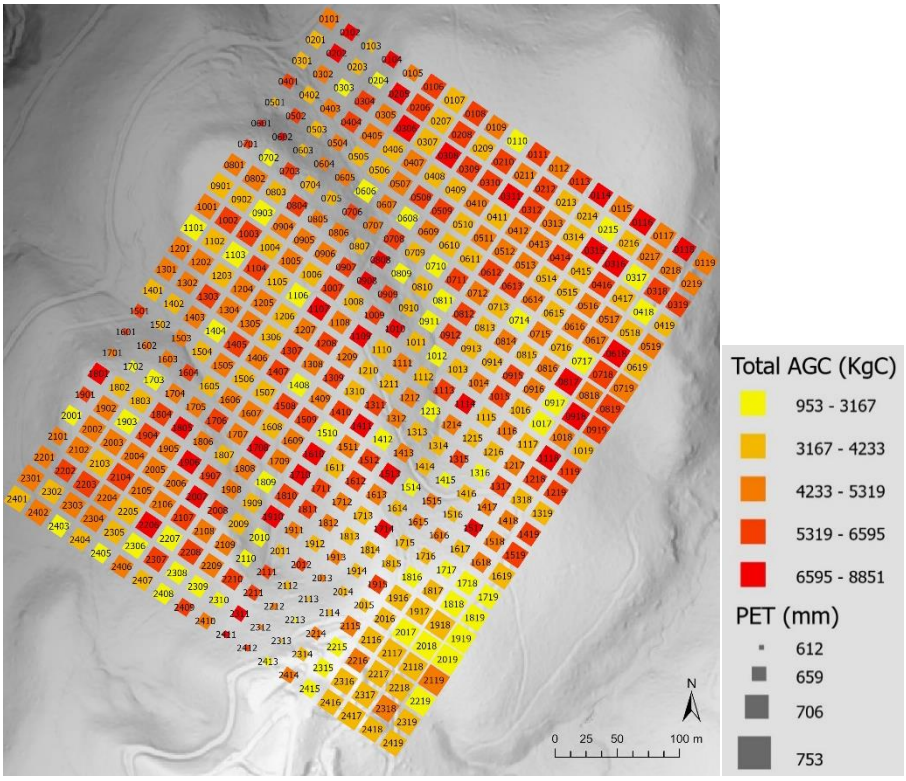

Figure S3: Bivariate display of above ground carbon content with PET per sub-plot. The size of the point is dependent on the above ground carbon content where smaller squares are areas of lower amounts

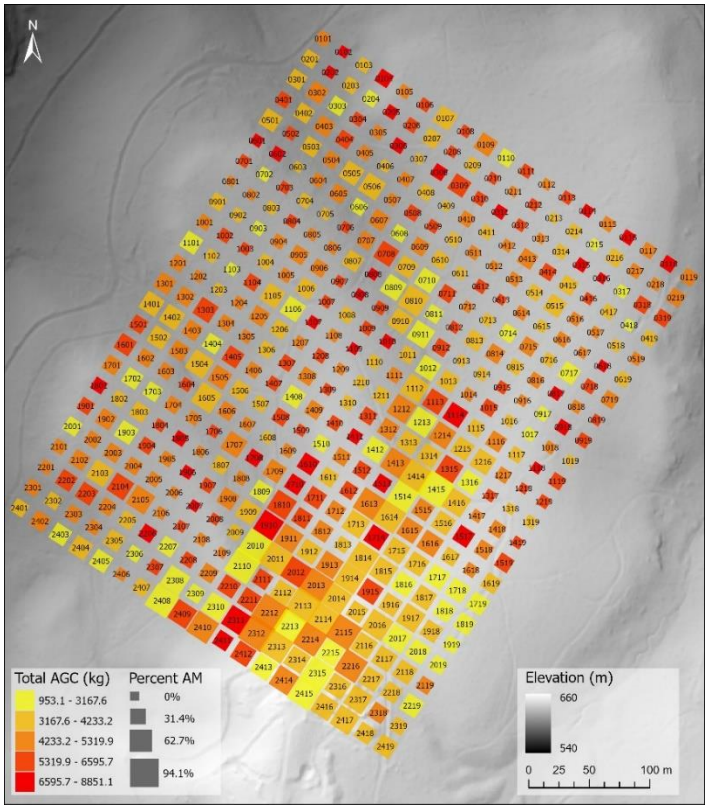

Figure S4: Bivariate display of above ground carbon with percent AM species per sub-plot

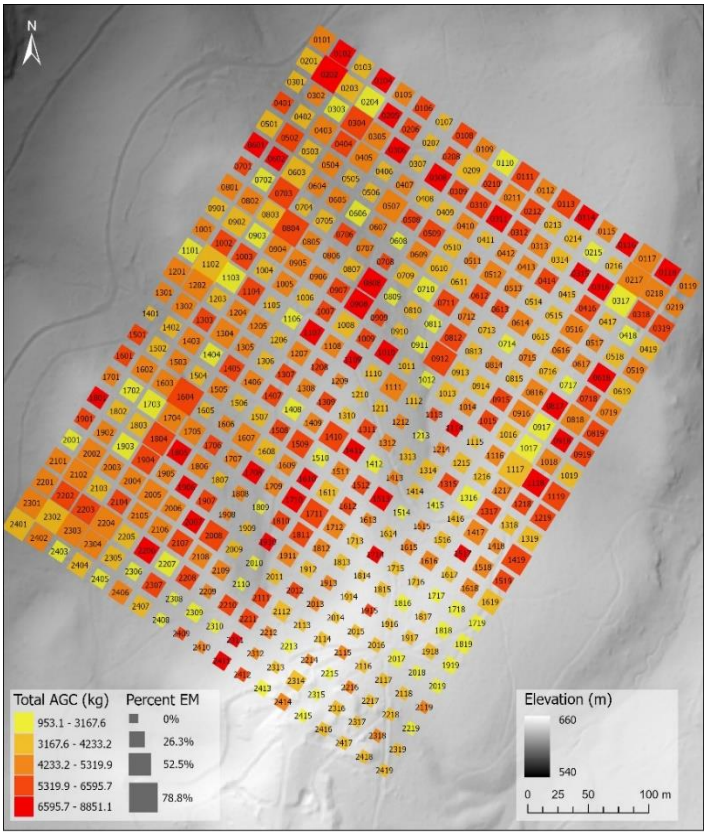

Figure S5: Bivariate display of above ground carbon with percent EM species per sub-plot

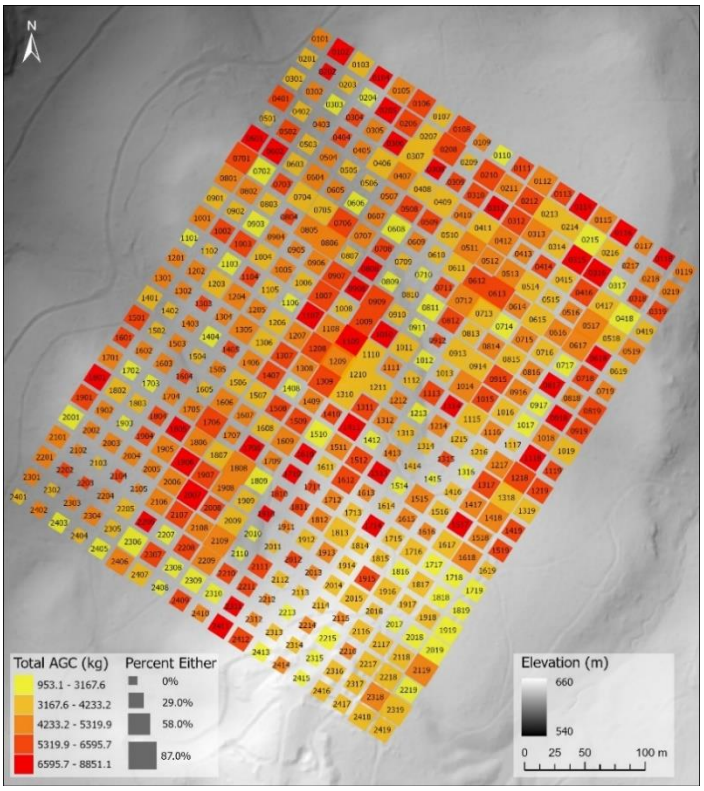

Figure S6: Bivariate display of above ground carbon percent red maple per sub-plot

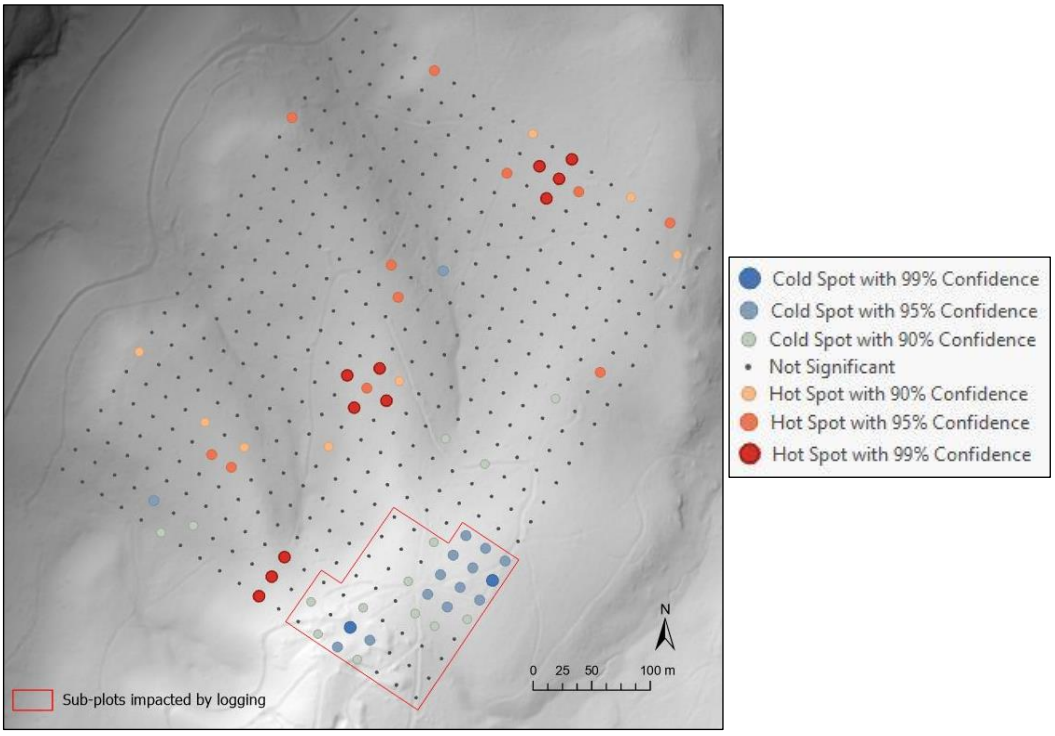

Figure S7: Hot spot analyses of above ground carbon with outlined logged region

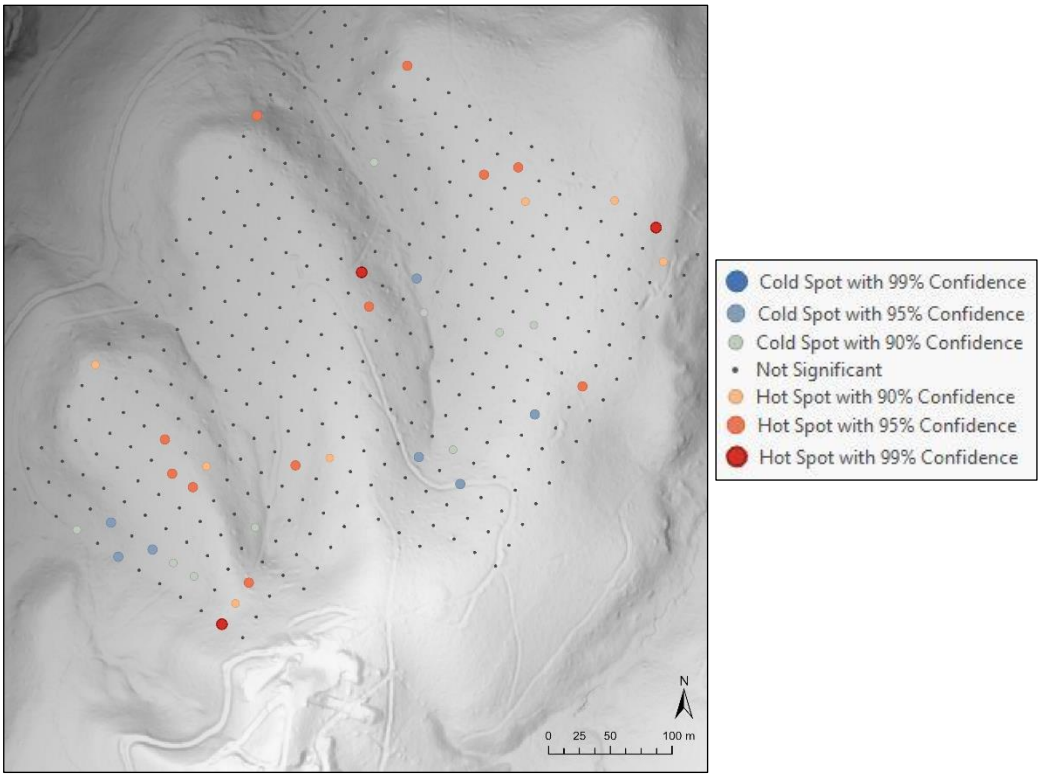

Figure S8: Hot spot analyses of above ground carbon with the logged region excluded

9. References

Abrams, M. D. (1998). The Red Maple Paradox. *BioScience*, *48*(5), 355–364. https://doi.org/10.2307/1313374

Alexander, H. D., Siegert, C., Brewer, J. S., Kreye, J., Lashley, M. A., McDaniel, J. K., Paulson, A. K., Renninger, H. J., & Varner, J. M. (2021). Mesophication of oak landscapes: Evidence, knowledge gaps, and future research. *BioScience*, *71*(5), 531–542. https://doi.org/10.1093/biosci/biaa169

Beck, D. E., & Hooper, R. M. (1986). Development of a southern appalachian hardwood stand after clearcutting. *Southern Journal of Applied Forestry*, *10*(3), 168–172. https://doi.org/10.1093/sjaf/10.3.168

Brice, M. H., Vissault, S., Vieira, W., Gravel, D., Legendre, P., & Fortin, M. J. (2020). Moderate disturbances accelerate forest transition dynamics under climate change in the temperate–boreal ecotone of eastern North America. *Global Change Biology*, *26*(8), 4418–4435. https://doi.org/10.1111/gcb.15143

Brundrett, M. C., & Tedersoo, L. (2020). Resolving the mycorrhizal status of important northern hemisphere trees. *Plant and Soil*, *454*(1-2), 3–34. https://doi.org/10.1007/s11104-020-04627-9

Canham, C. D., Papaik, M. J., Uriarte, M., McWilliams, W. H., Jenkins, J. C., & Twery, M. J. (2006). Neighborhood analyses of canopy tree competition along environmental gradients in New England forests. *Ecological Applications*, *16*(2), 540–554. https://doi.org/10.1890/1051-0761(2006)016[0540:naoctc]2.0.co;2

Chave, J., Coomes, D., Jansen, S., Lewis, S. L., Swenson, N. G., & Zanne, A. E. (2009). Towards a worldwide wood economics spectrum. *Ecology Letters*, *12*(4), 351–366. https://doi.org/10.1111/j.1461-0248.2009.01285.x

Chojnacky, D. C., Heath, L. S., & Jenkins, J. C. (2013). Updated generalized biomass equations for North American tree species. *Forestry*, *87*(1), 129–151. https://doi.org/10.1093/forestry/cpt053

Cheeke, T. E., Phillips, R. P., Brzostek, E. R., Rosling, A., Bever, J. D., & Fransson, P. (2016). Dominant mycorrhizal association of trees alters carbon and nutrient cycling by selecting for microbial groups with distinct enzyme function. *New Phytologist*, *214*(1), 432–442. https://doi.org/10.1111/nph.14343

Crowther, T. W., Glick, H. B., Covey, K. R., Bettigole, C., Maynard, D. S., Thomas, S. M., Smith, J. R., Hintler, G., Duguid, M. C., Amatulli, G., Tuanmu, M.-N., Jetz, W., Salas, C., Stam, C., Piotto, D., Tavani, R., Green, S., Bruce, G., Williams, S. J., … Bradford, M. A. (2015). Mapping tree density at a global scale. *Nature*, *525*(7568), 201–205. https://doi.org/10.1038/nature14967

Deskins, J. (2019). Economic Impact of the Summit Bechtel Family National Scout Reserve on West Virginia.

D'Orangeville, L., Maxwell, J., Kneeshaw, D., Pederson, N., Duchesne, L., Logan, T., Houle, D., Arseneault, D., Beier, C. M., Bishop, D. A., Druckenbrod, D., Fraver, S., Girard, F., Halman, J., Hansen, C., Hart, J. L., Hartmann, H., Kaye, M., Leblanc, D., … Phillips, R. P. (2018). Drought timing and local climate determine the sensitivity of eastern temperate forests to drought. *Global Change Biology*, *24*(6), 2339–2351. https://doi.org/10.1111/gcb.14096

Dye, A., Barker Plotkin, A., Bishop, D., Pederson, N., Poulter, B., & Hessl, A. (2016). Comparing tree-ring and permanent plot estimates of aboveground net primary production in three eastern U.S. forests. *Ecosphere*, *7*(9). https://doi.org/10.1002/ecs2.1454

Dyer, J. (2004). A water budget approach to predicting tree species growth and abundance, utilizing paleoclimatology sources. *Climate Research*, *28*, 1–10. https://doi.org/10.3354/cr028001

Dyer, J. M. (2009). Assessing topographic patterns in moisture use and stress using a water balance approach. *Landscape Ecology*, *24*(3), 391–403. https://doi.org/10.1007/s10980-008-9316-6

Dyer, J. M., & Hutchinson, T. F. (2019). Topography and soils-based mapping reveals fine-scale compositional shifts over two centuries within a central Appalachian Landscape. *Forest Ecology and Management*, *433*, 33–42. https://doi.org/10.1016/j.foreco.2018.10.052

Esri. "How Hot Spot Analysis (Getis-Ord Gi*) Works". (Accessed on May 15, 2023). ttps://pro.arcgis.com/en/pro-app/latest/tool-reference/spatial-statistics/h-how-hot-spot-analysis-getis-ord-gi-spatial-stati.htm#:~:text=The%20Hot%20Spot%20Analysis%20tool%20calculates%20the%20Getis-Ord,each%20feature%20within%20the%20context%20of%20neighboring%20features.

Fekedulegn, D., Hicks, R. R., & Colbert, J. J. (2003). Influence of topographic aspect, precipitation and drought on radial growth of four major tree species in an Appalachian watershed. *Forest Ecology and Management*, *177*(1-3), 409–425. https://doi.org/10.1016/s0378-1127(02)00446-2

Finzi, A. C., Giasson, M., Barker Plotkin, A. A., Aber, J. D., Boose, E. R., Davidson, E. A., Dietze, M. C., Ellison, A. M., Frey, S. D., Goldman, E., Keenan, T. F., Melillo, J. M., Munger, J. W., Nadelhoffer, K. J., Ollinger, S. V., Orwig, D. A., Pederson, N., Richardson, A. D., Savage, K., … Foster, D. R. (2020). Carbon budget of the Harvard Forest Long-Term ecological research site: Pattern, process, and response to global change. *Ecological Monographs*, *90*(4). https://doi.org/10.1002/ecm.1423

Fisher JB, DiBiase TA, Qi Y, Xu M, Goldstein AH (2005) Evapotranspiration models compared on a Sierra Nevada forest ecosystem. Environ Model Softw 20:783–796. doi: 10.1016/j.envsoft.2004.04.009

Gaertner, B. A., Zegre, N., Warner, T., Fernandez, R., He, Y., & Merriam, E. R. (2019). Climate, forest growing season, and evapotranspiration changes in the Central Appalachian Mountains, USA. *Science of The Total Environment*, *650*, 1371–1381. https://doi.org/10.1016/j.scitotenv.2018.09.129

Hanson, P. J., Todd, D. E., & Amthor, J. S. (2001). A six-year study of Sapling and large-tree growth and mortality responses to natural and induced variability in precipitation and throughfall. *Tree Physiology*, *21*(6), 345–358. https://doi.org/10.1093/treephys/21.6.345

Jenkins, C., Chojnacky, D., Heath, L., Birdsey, R., National-Scale Biomass Estimators for United States Tree Species, *Forest Science*, Volume 49, Issue 1, February 2003, Pages 12–35, https://doi.org/10.1093/forestscience/49.1.12

Mencuccini, M., Martinez-Vilalta, J., Vanderklein, D., Hamid, H. A., Michiels, B., Lee, S., & Korakaki, E. (2005). Size-mediated ageing reduces vigour in trees. *Ecology Letters*, *8*,1183–1190. https://doi.org/https://doi.org/10.1111/j.1461-0248.2005.00819.x

NOAA. "U.S. Climate Normals Quick Access". (Accessed on April 25, 2023). https://www.ncei.noaa.gov/access/us-climate-normals/#dataset=normals-monthly&timeframe=30&location=WV&station=USC00466591

Nowacki, G. J., & Abrams, M. D. (2008). The demise of fire and "mesophication" of forests in the Eastern United States. *BioScience*, *58*(2), 123–138. https://doi.org/10.1641/b580207

Piponiot, C., Anderson-Teixeira, K. J., Davies, S. J., Allen, D., Bourg, N. A., Burslem, D. F., Cárdenas, D., Chang-Yang, C. H., Chuyong, G., Cordell, S., Dattaraja, H. S., Duque, Á., Ediriweera, S., Ewango, C., Ezedin, Z., Filip, J., Giardina, C. P., Howe, R., Hsieh, C. F., … Muller-Landau, H. C. (2022). Distribution of biomass dynamics in relation to tree size in forests across the world. *New Phytologist*. https://doi.org/10.1111/nph.17995

Rygiewicz, P. T., & Andersen, C. P. (1994). Mycorrhizae alter quality and quantity of carbon allocated below ground. *Nature*, *369*(6475), 58–60. https://doi.org/10.1038/369058a0

Shen, X., Gatto, P., & Pagliacci, F. (2023). Unravelling the role of institutions in market-based instruments: A systematic review on Forest Carbon Mechanisms. *Forests*, *14*(1), 136. https://doi.org/10.3390/f14010136

Smith, J. E., Heath, L. S., & Woodbury, P. B. (2004). How to Estimate Forest Carbon for Large Areas from Inventory Data. *Journal of Forestry*, *102*(5), 25–31. https://doi.org/https://doi.org/10.1093/jof/102.5.25

Soudzilovskaia, N. A., van Bodegom, P. M., Terrer, C., Zelfde, M. van't, McCallum, I., Luke McCormack, M., Fisher, J. B., Brundrett, M. C., de Sá, N. C., & Tedersoo, L. (2019). Global mycorrhizal plant distribution linked to terrestrial carbon stocks. *Nature Communications*, *10*(1). https://doi.org/10.1038/s41467-019-13019-2

Soil Survey Staff. The Gridded Soil Survey Geographic (SSURGO) Database for West Virginia. United States Department of Agriculture, Natural Resources Conservation Service. Available online at https://gdg.sc.egov.usda.gov/. November 17, 2020 (202007 official release).

Soil Survey Staff. National Value Added Look Up (Valu1) Table for the Gridded Soil Survey Geographic (gSSURGO) Database for the United States of America and the Territories, Commonwealths, and Island Nations served by the USDA-NRCS. United States Department of Agriculture, Natural Resources Conservation Service. Available online at https://gdg.sc.egov.usda.gov/. 10, 30, 2022.

Soil Survey Staff, Natural Resources Conservation Service, United States Department of Agriculture. Web Soil Survey. Available online at the following link: http://websoilsurvey.sc.egov.usda.gov/. *Accessed [03/27/2023]*.

"Summit Bechtel Reserve." 37°54'22.92"N and 81° 6'24.42"W. GOOGLE EARTH. April 1996. March 6, 2023.

USDA & NRCS. 2023. The PLANTS Database (http://plants.usda.gov, 06/14/2023). National Plant Data Team, Greensboro, NC USA.

Van Kooten, G. C., & Johnston, C. M. T. (2016). The economics of Forest Carbon Offsets. *Annual Review of Resource Economics*, *8*(1), 227–246. https://doi.org/10.1146/annurev-resource-100815-095548

Ward, E. B., Duguid, M. C., Kuebbing, S. E., Lendemer, J. C., Warren, R. J., & Bradford, M. A. (2021). Ericoid mycorrhizal shrubs alter the relationship between tree mycorrhizal dominance and soil carbon and nitrogen. *Journal of Ecology*, *109*(10), 3524–3540. https://doi.org/10.1111/1365-2745.13734

Xu, X., Dimitrov, D., Shrestha, N., Rahbek, C., & Wang, Z. (2019). A consistent species richness–climate relationship for Oaks across the Northern Hemisphere. *Global Ecology and Biogeography*. https://doi.org/10.1111/geb.12913

Zanne, Amy E. et al. (2009), Data from: Towards a worldwide wood economics spectrum, Dryad, Dataset, https://doi.org/10.5061/dryad.234